LETTERS
PUBLISHED ONLINE: 16 NOVEMBER 2015 | DOI: 10.1038/NPHOTON.2015.214
nature photonics

Capacity limits of spatially multiplexed free-space communication

Ningbo Zhao[1], Xiaoying Li[1], Guifang Li[1,2]* and Joseph M. Kahn[3]*

Increasing the information capacity per unit bandwidth has been a perennial goal of scientists and engineers[1]. Multiplexing of independent degrees of freedom, such as wavelength, polarization and more recently space, has been a preferred method to increase capacity[2,3] in both radiofrequency and optical communication. Orbital angular momentum, a physical property of electromagnetic waves discovered recently[4], has been proposed as a new degree of freedom for multiplexing to achieve capacity beyond conventional multiplexing techniques[5–9], and has generated widespread and significant interest in the scientific community[10–14]. However, the capacity of orbital angular momentum multiplexing has not been established or compared to other multiplexing techniques. Here, we show that orbital angular momentum multiplexing is not an optimal technique for realizing the capacity limits of a free-space communication channel[15–17] and is outperformed by both conventional line-of-sight multi-input multi-output transmission and spatial-mode multiplexing.

An orbital angular momentum (OAM) mode carrying angular momentum $l\hbar$ in free space is a Laguerre–Gaussian (LG) beam given by

$$E_{pl}(r,\phi) = \sqrt{\frac{2p!}{\pi(p+|l|)!}}\frac{1}{w_0}\left[\frac{r\sqrt{2}}{w_0}\right]^{|l|}\exp\left(\frac{-r^2}{w_0^2}\right)L_p^{|l|}\left(\frac{2r^2}{w_0^2}\right)e^{il\phi} \quad (1)$$

where p is the radial index, r is the radius, φ is the azimuth angle, $L_p^{|l|}$ is the Laguerre polynomial and w_0 is the waist size of the OAM mode with $l=0$, $p=0$, which is the fundamental Gaussian mode. As can be seen from the last factor in equation (1), the integer OAM number l indicates the rate of azimuthal twist of the phase front. This is why OAM modes have been referred to as twisted photons or twisted radio waves[14,16]. Because OAM is only conserved when a beam traverses systems with central rotational symmetry, OAM multiplexing cannot be used reliably in off-axis wireless communication, wireless communication with multiple scattering, or in fibre-optic communication, where a fibre's rotational symmetry cannot be maintained reliably over long distances. Hence, OAM multiplexing has been applied mainly to near-field line-of-sight (LOS) free-space communication.

Within the context of LOS communication, it has been argued that OAM multiplexing potentially provides infinite spectral efficiency (SE) or information capacity, because the OAM number can take on arbitrarily large (quantized) values[5,10]. As a result, there has been a flurry of efforts towards the generation[18–20], manipulation[21,22] and detection[23] of OAM for communications. However, others have argued that OAM multiplexing is only a subset of the solutions offered by multi-input multi-output (MIMO) transmission[11,12] and cannot provide SE gain in the far field[14]. The purpose of this Letter is to provide a rigorous comparison between the capacity of OAM multiplexing and that of systems using conventional LOS MIMO or spatial-mode multiplexing (SMM).

To provide a framework for a fair comparison, we first define a canonical LOS system, as shown in Fig. 1a. This comprises a transmitter aperture, and a free-space transmission channel including a single thin positive lens and a receiver aperture, all circular and aligned along a common central axis. To simplify the analysis, we assume that the aperture sizes and numerical apertures (or equivalently, the antenna gains) on the transmitter and receiver sides are identical. The canonical system is low-pass in terms of transverse spatial frequencies, with maximum input angle Θ or numerical aperture NA = $\sin\Theta$ and thus maximum transverse spatial frequency $k_0 \times \mathrm{NA}$, where $k_0 = 2\pi/\lambda$ and λ is the wavelength. The transmitter and receiver planes are confined to circles of finite radius R_0. We can therefore conveniently describe the physical resources of the LOS wireless channel by a dimensionless space–bandwidth product (SBP) $2R_0 \times 2\mathrm{NA}/\lambda$. As shown in Supplementary Section 1, this canonical single-lens system, with appropriate choice of focal length and aperture size, can represent any system using either a single lens or separate lenses at the transmitter and receiver, whether identical or different, provided it is properly designed to nominally avoid beam clipping. The single-lens canonical system can also describe a fibre with a parabolic index profile.

In OAM multiplexing, information is transmitted using beams with a common central rotational axis but different angular momenta, corresponding to different values of l. A fixed OAM number l can be provided by any of the mth-order ($m = 2p + |l| + 1$) LG modes, which have root-mean-squared (r.m.s.) waist sizes[24] of $w_m = \sqrt{m}w_0$ and divergence angles of $\theta_m = \sqrt{m}\theta_0$, where θ_0 is the divergence of the fundamental Gaussian mode and $w_m\theta_m/\lambda = mw_0\theta_0/\lambda = m/\pi$, which can be interpreted as the space–bandwidth product of the OAM mode. The beam divergence and beam waist (aperture size) cannot be scaled independently for a system with a fixed SBP. Because, for a given l, the OAM mode with $p=0$ has the minimum SBP, OAM-multiplexed systems investigated to date have used the LG_{0l} modes[5,7]. At the receiver, we consider two scenarios. In the first, the OAM modes are demultiplexed without loss or crosstalk using OAM sorting elements[25–27] and subsequently detected coherently. In the second scenario, the OAM modes are demultiplexed using the same conventional MIMO technique as for LOS MIMO and SMM, as described in the next paragraph.

In conventional LOS MIMO, the transmitter aperture is subdivided into smaller circular apertures packed in a honeycomb formation (Fig. 1b), each transmitting an independent fundamental Gaussian beam. The receiver aperture is divided into smaller hexagons in a honeycomb formation to maximize the fill factor and thus minimize loss (Fig. 1c). Signals arriving at each hexagon are detected coherently.

In SMM, the transmitter aperture is similar to that for OAM multiplexing, but it transmits a complete set of spatial modes, such as all the LG modes LG_{pl}, including those with $p \neq 0$, that are not used in OAM

[1]Key Laboratory of Optoelectronics Information Technology of Ministry of Education, College of Precision Instrument and Opto-Electronic Engineering, Tianjin University, Tianjin, China. [2]CREOL, The College of Optics & Photonics, University of Central Florida, Orlando, Florida 32816-2700, USA.
[3]Edward L. Ginzton Laboratory, Stanford University, 348 Via Pueblo Mall, Stanford, California 94305-4088, USA. *e-mail: li@ucf.edu; jmk@ee.stanford.edu

multiplexing. SMM is the free-space counterpart of the mode-division multiplexing (MDM) currently being investigated for fibre-optic communication[28]. In fact, multiplexing techniques developed for MDM can be used for the generation and demultiplexing of SMM signals, as shown in Supplementary Section 3. Equivalently, the zero-OAM Hermite–Gaussian (HG) modes of the form

$$E_{n_x n_y}(x,y) = u_{n_x}(x)u_{n_y}(y),\ u_{n_x}(x) = \left(\frac{2}{\pi}\right)^{1/4}\left(\frac{1}{2^n n_x! w_0}\right)^{1/2} H_{n_x}\left(\frac{\sqrt{2}x}{w}\right) \quad (2)$$

can be used for SMM, where $n_{x/y}$ are the indices for the x/y direction and H_{n_x} is the Hermite polynomial. Both the LG and HG mode sets represent complete bases for free-space electromagnetic waves, while OAM modes are a subset of a complete basis. The LG modes and HG modes are related by a unitary transformation. The receiver used for SMM is the same as for conventional LOS MIMO.

Let the transmitted and received signals at time t be

$$\mathbf{s}(t) = [s_1(t)s_2(t)\cdots s_M(t)]^T \quad (3)$$

and

$$\mathbf{r}(t) = [r_1(t)r_2(t)\cdots r_M(t)]^T$$

As the free-space channel is linear, the input and output are related by a transmission matrix $\mathbf{h}$ so that

$$\mathbf{r}(t) = \mathbf{h}\cdot\mathbf{s}(t) \quad (4)$$

Because of the limited SBP of the LOS system, the transmission matrix $\mathbf{h}$ will have loss and crosstalk. An information-theoretic limit to the SE of the LOS system, measured in bit s^{-1} Hz^{-1}, is given by[29]

$$\mathrm{SE} = \sum_{q=1}^{Q}\log_2\left(1+\lambda_q\frac{P_q}{\sigma^2}\right) \quad (5)$$

where λ_q are the squares of the singular values of the transmission matrix $\mathbf{h}$, λ_q are the eigenvalues of $\mathbf{h}^\dagger\mathbf{h}$, representing the gain of the corresponding subchannel, P_q is the power transmitted in the qth singular vector, or subchannel, of the transmission matrix, and σ^2 is the noise variance in each receiver element. As can be seen from equation (5), given a fixed receiver noise variance σ^2 and a fixed total transmitter power $P = \sum_{q=1}^{Q} P_q$, the SE is determined by Q, the number of independently addressable spatially multiplexed subchannels, and by λ_q, the gains of these subchannels. Our goal is to compare the SE given by equation (5) for the three multiplexing methods: OAM multiplexing, LOS MIMO and SMM, with the same physical resource constraints. Equation (5) assumes that the transmitter has knowledge of the Q singular vectors and their singular values, and allocates power to them optimally (see Methods).

To obtain an intuitive estimate of the number of independently addressable spatial subchannels Q, we may count the number of modes that fit into the SBP of the LOS system, $2R_0\times 2\mathrm{NA}/\lambda$, using equations (1) and (2) for OAM and SMM, respectively. We define a dimensionless parameter

$$M = \pi R_0\times \mathrm{NA}/\lambda$$

which is $\pi/4$ times the SBP and is the maximum order of LG modes supported by the SBP. The radii of the transmitter/receiver aperture and the numerical aperture are assumed to be $R_0 = \sqrt{M}w_0$ and $\mathrm{NA} = \sin(\sqrt{M}\theta_0)$, respectively. Such a choice optimally utilizes the space and bandwidth resources because of the inherent relationship between the beam waist and beam divergence.

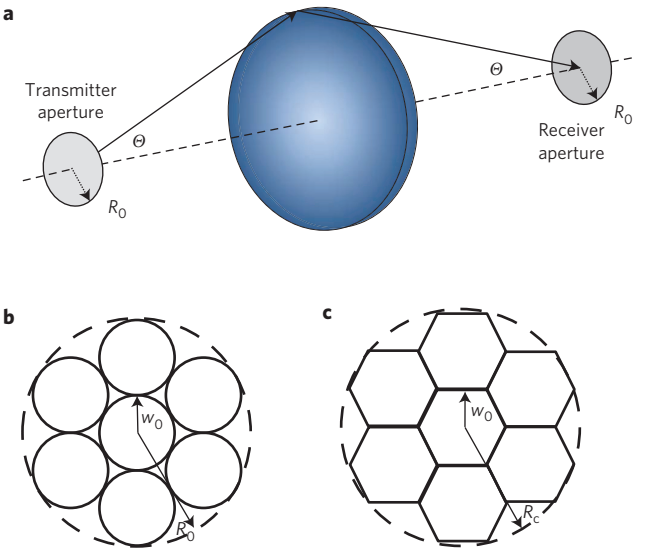

Figure 1 | Schematic of transmission systems. a, Schematic of a canonical LOS system. **b**, Transmitter arrangement for conventional LOS MIMO, where each small circle represents one of the parallel beams. **c**, Receiver arrangement, where the receiver aperture is divided into hexagonal cells to maximize the fill factor.

For OAM multiplexing, the number of independently addressable spatial subchannels is estimated to be

$$Q_{\mathrm{OAM}} \approx 2M+1 \quad (6)$$

corresponding to the number of LG modes with $p = 0$.

For SMM using LG modes, the number of independently addressable spatial subchannels can be estimated as

$$Q_{\mathrm{SMM}} \geq \frac{1}{2}M(M+1) \quad (7a)$$

counting all permutations of p and l that satisfy $2p+|l|+1\leq M$. Equation (7a) is a lower bound, as the r.m.s. waist of an LG mode is larger than the largest radius of its local intensity maximum[24]. Alternatively, we can use the condition that the largest radius of the local intensity minimum should be less than R_0. This allows the LG mode order to increase from M to $16M/\pi^2$ and, as a result, upper bounds the number of independently addressable spatial subchannels by

$$Q_{\mathrm{SMM}} \leq \frac{128}{\pi^4}M(M+1) = 1.314M(M+1) \quad (7b)$$

The best estimate of Q for SMM lies between equations (7a) and (7b). Manual counting of the number of LG modes with the largest radius of the local field/intensity maximum less than R_0 yields an approximation (with <1% error for $M>9$),

$$Q_{\mathrm{SMM}} \approx \frac{1}{\sqrt{2}}(M+7)(M-1) \quad (7c)$$

Because HG modes and LG modes are related by a unitary transformation, the two sets of modes yield the same number of independently addressable spatial subchannels, as estimated by equations (7a) to (7c).

For conventional MIMO, analytical solutions exist only for rectangular apertures using the Nyquist sampling theorem[30]. For circular apertures, we can obtain an approximate bound as follows. Each Gaussian beam can have a divergence angle as large as that for the

Mth-order LG mode above. Consequently, each Gaussian beam has a waist size of $w = w_0/\sqrt{M}$, which is M times smaller than the Mth-order OAM mode above. The question of how many independently addressable MIMO subchannels can be supported by the SBP is equivalent to how many circles of radius $w_0/\sqrt{M}$ can fit into a large circle of radius $\sqrt{M}w_0$. An analytical solution for such a packing problem does not exist. However, it is known that in the limit of large M, the approximate number of independently addressable MIMO subchannels is upper-bounded as[31]

$$Q_{\mathrm{LOS}} \leq 0.9M^2 \tag{8}$$

A comparison of equations (6), (7a) to (7c) and (8) indicates that OAM multiplexing is expected to have the smallest number of independently addressable subchannels among the three multiplexing methods for a given SBP.

As shown in equation (5), the SE of a multiplexed system not only depends on the number of independently addressable subchannels Q, but also on the singular values of the transmission matrix. To compare the SE of the three multiplexing methods rigorously, we simulate beam propagation and coherent detection (see Methods) to determine the singular values, SE and effective degrees of freedom (EDOF), which represents the number of subchannels that are actively conveying information for the three multiplexing techniques under consideration. In obtaining the simulation results given below, the only approximation we used was the paraxial approximation. System configurations for the highest SBP considered below that satisfy the paraxial approximation are given in Supplementary Section 1.

In OAM multiplexing, because the system has central rotational symmetry, OAM is conserved but power is lost due to diffraction. The transmission matrix for OAM multiplexing is therefore diagonal and non-unitary, assuming a perfect OAM demultiplexer[26,27] that introduces no loss or crosstalk. Diffraction is the only effect included in the simulation for OAM using a perfect demultiplexer. So, the results for OAM with perfect demultiplexing represent an upper bound for the SE of OAM multiplexing.

For conventional LOS MIMO and SMM, every received subchannel not only suffers loss due to diffraction, but is also subject to crosstalk from other subchannels, due to diffraction and the design of the MIMO demultiplexer (Fig. 1c). Hence, the transmission matrices are non-diagonal and non-unitary. We also consider OAM transmission with demultiplexing performed by the MIMO demultiplexer, in which case the transmission matrix is non-diagonal and non-unitary.

Figure 2 shows the singular values of the transmission matrix in descending order for the three multiplexing methods for $M = 3$, 9 and 21. It is seen that OAM multiplexing has larger singular values than the other two methods when the SBP is small (Fig. 2a), but has much smaller singular values than the other two methods when the SBP is large (Fig. 2b,c). Figure 3 shows the SE and the EDOF for the three multiplexing methods for $M = 3$, 9 and 21 as a function of the system signal-to-noise ratio (SNR), $\mathrm{SNR} = P/\sigma^2$ where P is the total transmitter power and σ^2 is the receiver noise power per subchannel. Transmitter powers corresponding to the SNR values considered for the optical and microwave/millimetre-wave regimes are given in Supplementary Section 2. The EDOFs at high transmitted powers are in good agreement with estimates of the number of independent subchannels Q, given by equations (6), (7c) and (8), for all three multiplexing methods. Although the three methods offer similar SEs and EDOFs for small SBPs (Fig. 3a,d), SMM and conventional LOS MIMO offer much higher SEs and EDOFs than OAM multiplexing for large SBPs (Fig. 3c,f), particularly at moderate to high SNRs.

Both conventional LOS MIMO and SMM exploit the two degrees of freedom (x,y) or (r,θ) of the transmitter/receiver apertures, while OAM multiplexing only exploits the azimuthal DOF (θ) of the transmitter/receiver apertures. When the SBP is high,

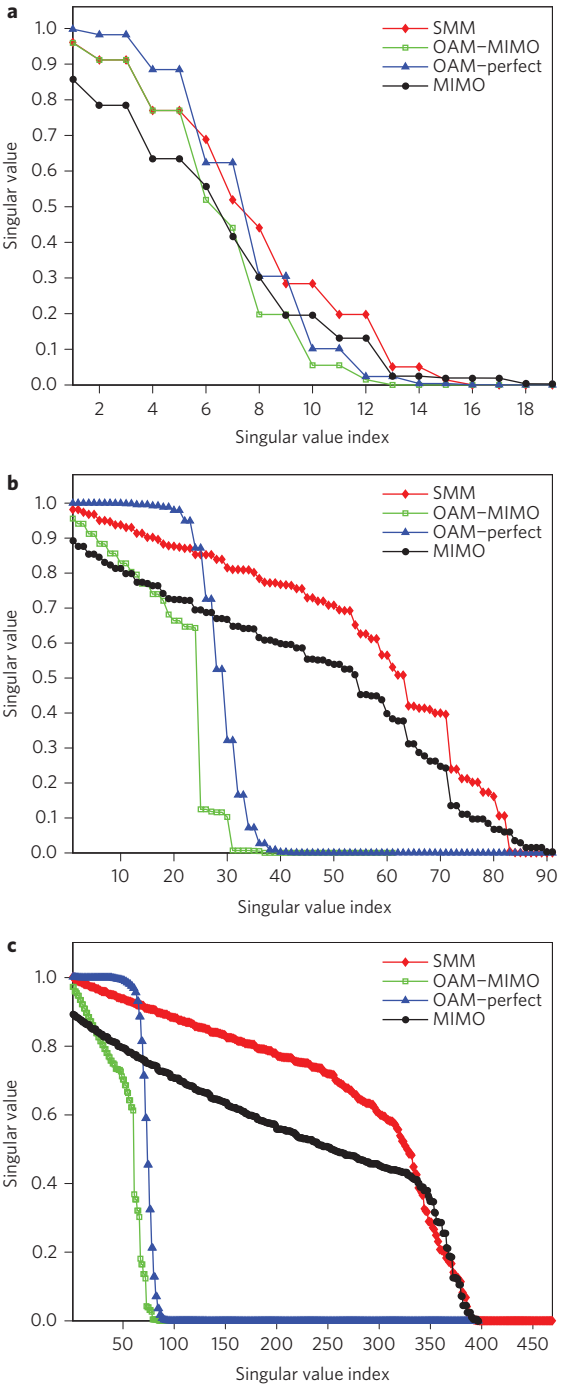

Figure 2 | Comparison of singular values of the transmission matrix in descending order for different multiplexing/demultiplexing methods. **a**–**c**, Singular values for $M = 3$ (**a**), $M = 9$ (**b**) and $M = 21$ (**c**). SMM and conventional LOS MIMO have much larger singular values than OAM when the SBP is large, as in **b** and **c**.

conventional LOS MIMO and SMM achieve higher SEs and EDOFs than OAM multiplexing.

Based on the results presented above, we can make the following conclusions. First, SMM is the best multiplexing technique for realizing the ultimate SE or capacity that can be supported by the physical resources of an LOS communication system. Second, OAM multiplexing may be useful in LOS communication when the SBP is small, but only under unlikely and idealized conditions. This is because the first three lowest-order OAM modes and the

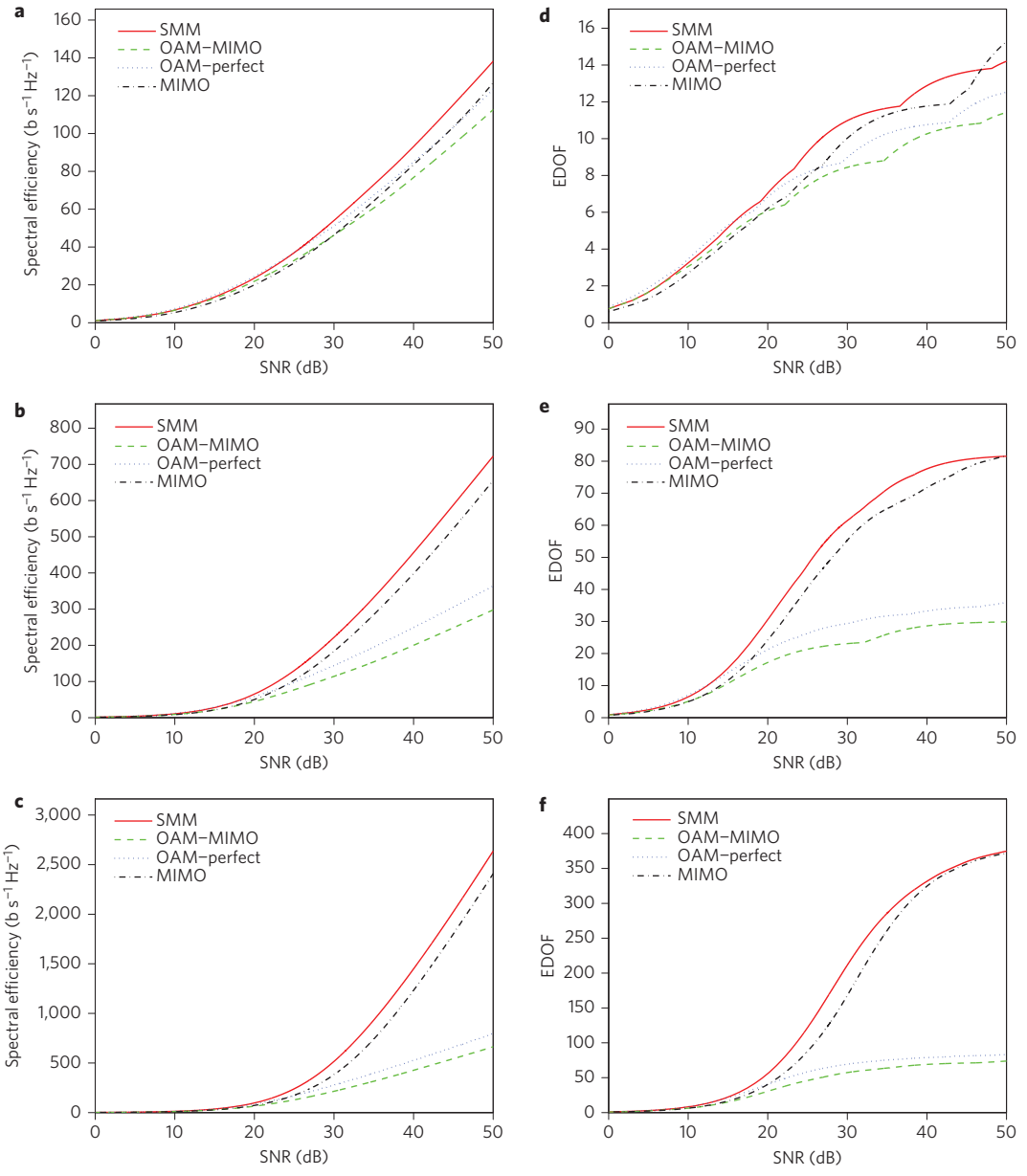

Figure 3 | Spectral efficiencies and effective degrees of freedom (EDOF) for different multiplexing/demultiplexing methods. a–c, Spectral efficiencies with $M = 3$ (**a**), $M = 9$ (**b**) and $M = 21$ (**c**). **d–f**, EDOF with $M = 3$ (**d**), $M = 9$ (**e**) and $M = 21$ (**f**). SMM and conventional LOS MIMO offer much larger spectral efficiencies and EDOF for large SBPs, as in **c** and **f**.

first three lowest-order HG modes are related by a lossless unitary transformation. Both sets of modes can exploit the available degrees of freedom. Because previous research on OAM has yielded effective methods for demultiplexing without requiring subsequent MIMO signal processing[26,27], OAM multiplexing may be the simplest method to achieve maximal SE with small SBPs. However, we should caution that this is only true if the alignment of the LOS system is perfect. As shown in Supplementary Section 4, OAM multiplexing is more sensitive to misalignment than SMM or conventional LOS MIMO. In addition, OAM multiplexing using optical demultiplexing is susceptible to turbulence because, in general, propagation through turbulence does not preserve OAM. A previous study found a severe crosstalk penalty (10 dB) for OAM multiplexing in weak to medium turbulence[32]. Third, conventional LOS MIMO achieves nearly the same SE as SMM, yet it requires the simplest transmitter architecture among the three multiplexing methods. It is expected that conventional LOS MIMO should experience the lowest multiplexing loss, as it does not require a multiplexer. So, conventional LOS MIMO may offer the best capacity–cost tradeoff of the three methods considered.

The comparison made here between OAM and SMM, while performed for free-space propagation, is also applicable to fibres with idealiszd parabolic index profiles, because propagation in such fibres can be described by the canonical LOS system described above, as shown in Supplementary Section 1. In such fibres, the SBP is described by a dimensionless normalized frequency V, which is equal to twice the dimensionless parameter M defined above, if we equate the fibre core radius to the transmitter/receiver radius R_0 defined in the canonical LOS system. Given a fibre with a certain value of V, the number of independently addressable spatial subchannels Q per polarization corresponds to the number of propagating spatial modes, which can be estimated for OAM or SMM using equations (6) and (7), replacing M by $V/2$. We thus

conclude that in fibres, as in free space, OAM multiplexing achieves smaller SE and EDOF than SMM.

Thus far, we have considered transmission in a single polarization. Transmitting independent information in two polarizations can double the SE for all schemes considered here. SMM with polarization multiplexing is the same as the MDM currently being studied extensively in optical fibre[33]. MDM in fibre or free space can use different modal bases, such as linearly polarized (LP) modes or vector modes. The modes considered here represent the spatial part of LP modes. The LP modes are linear combinations of the vector modes. At any given SBP, the number of LP modes in two polarizations is the same as the number of vector modes, so using vector modes does not increase capacity.

More generally, the key quantity of interest in any communication system, whether classical or quantum, whether in free space or in fibre, is the number of DOF. OAM is not a new DOF; OAM modes are a subset of the LG modes, which are equivalent to linear combinations of the zero-OAM HG modes. Any advantage that may exist for OAM modes can also be exploited using these other sets of modes. When choosing a basis set for communications, one should consider first whether the set is complete, and second how convenient the set is for implementation in the application at hand, regardless of whether the basis set includes OAM modes. OAM modes should be considered a preferred basis only when angular momentum is actually useful for the application at hand, for example, in light–matter interactions.

Methods

Methods and any associated references are available in the online version of the paper.

Received 18 May 2015; accepted 2 October 2015; published online 16 November 2015; corrected after print 27 November 2015

References

1. Shannon, C. E. A mathematical theory of communication. *Bell Syst. Tech. J.* **23,** 45 (1948).
2. Ng, S. X. , Hanzo, L. L., Keller, T. & Webb, W. *Quadrature Amplitude Modulation: From Basics to Adaptive Trellis-Coded, Turbo-Equalised and Space–Time Coded OFDM, CDMA and MC-CDMA Systems* (Wiley-IEEE, 2004).
3. Evangelides, S. G. Jr, Mollenauer, L. F., Gordon, J. P. & Bergano, N. S. Polarization multiplexing with solitons. *J. Lightw. Technol.* **10,** 28–35 (1992).
4. Allen, L., Beijersbergen, M. W., Spreeuw, R. J. C. & Woerdman, J. P. Orbital angular momentum of light and the transformation of Laguerre–Gaussian laser modes. *Phys. Rev. A* **45,** 8185–8189 (1992).
5. Fabrizio, T. *et al.* Encoding many channels on the same frequency through radio vorticity: first experimental test. *New J. Phys.* **14,** 033001 (2012).
6. Willner, A. E., Wang, J. & Huang, H. A different angle on light communications. *Science* **337,** 655–656 (2012).
7. Wang, J. *et al.* Terabit free-space data transmission employing orbital angular momentum multiplexing. *Nature Photon.* **6,** 488–496 (2012).
8. Yan, Y. *et al.* High-capacity millimetre-wave communications with orbital angular momentum multiplexing. *Nature Commun.* **5,** 4876 (2014).
9. Bozinovic, N. *et al.* Terabit-scale orbital angular momentum mode division multiplexing in fibers. *Science* **340,** 1545–1548 (2013).
10. Cartiledge, E. Adding a twist to radio technology: spiralling radio waves could revolutionize telecommunications. *Nature* http://dx.doi.org/10.1038/news.2011.114 (2011).
11. Edfors, O. & Johansson, A. J. Is orbital angular momentum (OAM) based radio communication an unexploited area? *IEEE Trans. Antennas Propag.* **60,** 1126–1131 (2012).
12. Michele, T., Christophe, C. & Julien, P.-C. Comment on 'Reply to Comment on "Encoding many channels on the same frequency through radio vorticity: first experimental test" '. *New J. Phys.* **15,** 078001 (2013).
13. Tamburini, F. *et al.* Reply to Comment on "Encoding many channels on the same frequency through radio vorticity: first experimental test". *New J. Phys.* **14,** 118002 (2012).
14. Kish, L. B. & Nevels, R. D. Twisted radio waves and twisted thermodynamics. *PLoS ONE* **8,** e56086 (2013).
15. Mair, A., Vaziri, A., Weihs, G. & Zeilinger, A. Entanglement of the orbital angular momentum states of photons. *Nature* **412,** 313–316 (2001).
16. Molina-Terriza, G., Torres, J. P. & Torner, L. Twisted photons. *Nature Phys.* **3,** 305–310 (2007).
17. Saleh, M. F., Di Giuseppe, G., Saleh, B. E. A. & Teich, M. C. Photonic circuits for generating modal, spectral, and polarization entanglement. *IEEE Photon. J.* **2,** 736–752 (2010).
18. Karimi, E. *et al.* Generating optical orbital angular momentum at visible wavelengths using a plasmonic metasurface. *Light Sci. Appl.* **3,** e167 (2014).
19. Xinlu, G. *et al.* Generating, multiplexing/demultiplexing and receiving the orbital angular momentum of radio frequency signals using an optical true time delay unit. *J. Opt.* **15,** 105401 (2013).
20. Cai, X. *et al.* Integrated compact optical vortex beam emitters. *Science* **338,** 363–366 (2012).
21. Strain, M. J. *et al.* Fast electrical switching of orbital angular momentum modes using ultra-compact integrated vortex emitters. *Nature Commun.* **5,** 4856 (2014).
22. Mirhosseini, M., Malik, M., Shi, Z. & Boyd, R. W. Efficient separation of the orbital angular momentum eigenstates of light. *Nature Commun.* **4,** (2013).
23. Genevet, P., Lin, J., Kats, M. A. & Capasso, F. Holographic detection of the orbital angular momentum of light with plasmonic photodiodes. *Nature Commun.* **3,** 1278 (2012).
24. Phillips, R. L. & Andrews, L. C. Spot size and divergence for Laguerre Gaussian beams of any order. *Appl. Opt.* **22,** 643–644 (1983).
25. O'Sullivan, M. N., Mirhosseini, M., Malik, M. & Boyd, R. W. Near-perfect sorting of orbital angular momentum and angular position states of light. *Opt. Express* **20,** 24444 (2012).
26. Lavery, M. P. J. *et al.* The efficient sorting of light's orbital angular momentum for optical communications. *Proc. SPIE* **8542,** 85421R (2012).
27. Berkhout, G. C. G., Lavery, M. P. J., Courtial, J., Beijersbergen, M. W. & Padgett, M. J. Efficient sorting of orbital angular momentum states of light. *Phys. Rev. Lett.* **105,** 153601 (2010).
28. Richardson, D. J., Fini, J. M. & Nelson, L. E. Space-division multiplexing in optical fibres. *Nature Photon.* **7,** 354–362 (2013).
29. Foschini, G. J. Layered space–time architecture for wireless communication in a fading environment when using multi-element antennas. *Bell Labs Tech. J.* **1,** 41–59 (1996).
30. Goodman, J. W. *Introduction to Fourier Optics* (McGraw Hill, 1996).
31. Wells, D. *The Penguin Book of Curious and Interesting Numbers Revised Edition* (Penguin, 1986).
32. Ren, Y. *et al.* Atmospheric turbulence effects on the performance of a free space optical link employing orbital angular momentum multiplexing. *Opt. Lett.* **38,** 4062–4065 (2013).
33. Li, G., Bai, N., Zhao, N. & Xia, C. Space-division multiplexing: the next frontier in optical communication. *Adv. Opt. Photon.* **6,** 413–487 (2014).

Acknowledgements

This work was supported in part by the National Key Basic Research Program of China (973), project #2014CB340104/3, NSFC projects 61377076, 61307085 and 61431009.

Author contributions

N.Z., G.L. and J.M.K. conceived and designed the theoretical model. N.Z. and X.L. performed the simulations. N.Z., G.L. and J.M.K. analysed the data. N.Z., G.L. and J.M.K. co-wrote the paper.

Additional information

Supplementary information is available in the online version of the paper. Reprints and permissions information is available online at www.nature.com/reprints. Correspondence and requests for materials should be addressed to G.L. and J.M.K.

Competing financial interests

The authors declare no competing financial interests.

Methods

Transmission matrix for OAM multiplexing. OAM multiplexing uses a subset of LG modes:

$$E_{0l}(r,\phi) = \sqrt{\frac{2}{\pi|l|!}}\frac{1}{w_0}\left[\frac{r\sqrt{2}}{w_0}\right]^{|l|}\exp\left(\frac{-r^2}{w_0^2}\right)e^{il\phi} = E_{0l}(r)e^{il\phi} \quad (9)$$

where l is the OAM number and w_0 is the waist size of the fundamental mode. A mode's spatial frequency spectrum is given by the Fourier transform of equation (9):

$$F_{0l}(\rho,\theta) = 2\pi(-i)^l\exp(il\theta)\int_0^{R_0} rE_{0l}(r)J_{|l|}(2\pi r\rho)\mathrm{d}r = F_{0l}(\rho)\exp(il\theta) \quad (10)$$

where R_0 is the radius of the transmitter or receiver aperture. Only spatial frequencies less than $B = \mathrm{NA}/\lambda$ can pass through the lens shown in Fig. 1a to reach the receiver. Therefore, under the paraxial approximation, the field distribution at the receiver aperture is given by

$$G_{0l}(r,\phi) = 2\pi(-i)^l\exp(il\phi)\int_0^B \rho F_{0l}(\rho)J_{|l|}(2\pi r\rho)\mathrm{d}\rho = G_{0l}(r)\exp(il\phi) \quad (11)$$

Assuming an aligned LOS system that has central rotational symmetry, the OAM of the field is conserved. Therefore, under the assumption of perfect OAM demultiplexing, the transmission matrix is diagonal with matrix elements

$$h_{l,l} = \sqrt{\frac{2\pi\int_0^{R_0} r\left|G_{0l}(r)\right|^2\mathrm{d}r}{2\pi\int_0^{R_0} r\left|E_{0l}(r)\right|^2\mathrm{d}r}} \quad (12)$$

If the OAM multiplexed signals are received using the MIMO receiver, then the transmission matrix is given by

$$h_{i,l} = \frac{\int_{\Sigma_i} G_{0l}(r,\phi)\mathrm{d}s}{\sqrt{2\pi\int_0^{R_0} r\left|E_{0l}(r)\right|^2\mathrm{d}r}} \quad (13)$$

where the integration region Σ_i corresponds to the ith receiving hexagon.

Transmission matrix for conventional LOS MIMO. For every sub-aperture on the transmitter plane, a Gaussian beam of waist size $w = w_0/\sqrt{m}$ is used to transmit independent information. Because of diffraction, the beam arriving at the receiver plane is broadened and is no longer confined within the corresponding receiver sub-aperture. The field distribution at the transmitter sub-aperture along the central axis is given by

$$E_0(r) = \sqrt{\frac{2}{\pi}}\frac{1}{w}\exp\left(-\frac{r^2}{w^2}\right) \quad (14)$$

Its spatial frequency spectrum is given by

$$F_0(\rho) = 2\pi\int_0^{R_0} rE_0(r)J_0(2\pi r\rho)\mathrm{d}r \quad (15)$$

The field reaching the central receiver aperture is given by

$$G_0(r) = 2\pi\int_0^B \rho F_0(\rho)J_0(2\pi r\rho)\mathrm{d}\rho \quad (16)$$

The transmission matrix element between the central transmitter sub-aperture and the ith receiving hexagon is therefore given by

$$h_{i,0} = \frac{\int_{\Sigma_i} G_0(r)\mathrm{d}s}{\sqrt{2\pi\int_0^{R_0} r\left|E_0(r)\right|^2\mathrm{d}r}} \quad (17)$$

Under the paraxial approximation, the transmission channel is linear and shift-invariant. The field at the receiver plane due to the jth transmitter sub-aperture, $G_j(r)$, is simply a shifted version of $G_0(r)$. Hence, all elements of the transmission matrix can be obtained using equation (17).

Transmission matrix for HG or LG mode multiplexing. HG or LG mode multiplexing uses two spatial degrees of freedom—(x,y) or (ρ,ϕ)—in the transmitter and receiver planes. The field of an LG mode is given by

$$E_{pl}(r,\phi) = \sqrt{\frac{2p!}{\pi(p+|l|)!}}\frac{1}{w_0}\left[\frac{r\sqrt{2}}{w_0}\right]^{|l|}\exp\left(\frac{-r^2}{w_0^2}\right)L_p^{|l|}\left(\frac{2r^2}{w_0^2}\right)e^{il\phi} = E_{pl}(r)e^{il\phi} \quad (18)$$

where p is the radial index and l is the OAM number. Its spatial frequency spectrum is given by

$$F_{pl}(\rho,\theta) = 2\pi(-i)^l\exp(il\theta)\int_0^{R_0} rE_{pl}(r)J_{|l|}(2\pi r\rho)\mathrm{d}r \quad (19)$$

and the correspond field at the receiver plane is given by

$$G_{pl}(r,\phi) = 2\pi(-i)^l\exp(il\phi)\int_0^B \rho F_{pl}(\rho)J_{|l|}(2\pi r\rho)\mathrm{d}\rho \quad (20)$$

Therefore the element of the transmission matrix between LG mode (p,l) and sub-aperture i are given by

$$h_{i,(p,l)} = \frac{\int_{\Sigma_i} G_{pl}(r,\phi)\mathrm{d}s}{\sqrt{2\pi\int_0^{R_0} r\left|E_{pl}(r)\right|^2\mathrm{d}r}} \quad (21)$$

Because HG modes are linear combinations of the LG modes, their mode amplitudes are related by a unitary transformation U. Therefore, the transmission matrix for HG multiplexing is related to that of the LG mode multiplexing by

$$H_{\mathrm{HG}} = UH_{\mathrm{LG}}U^{\dagger} \quad (22)$$

and the singular values for the two multiplexing methods are the same.

Spectral efficiency and effective degrees of freedom. The maximum SE as a function of total input power P is calculated using the standard water-filling algorithm to allocate power to the subchannels of the transmission matrix such that in each subchannel $N_0/\lambda_q + P_q$ is the same for all active subchannels and zero for all idle subchannels, subject to a total input power constraint[34]. The EDOF represents the number of subchannels that are actively conveying information. For a single-channel system, the SE is given by $\mathrm{SE} = \log_2(1 + P/N_0)$. When the total system power is increased by a factor K, the system SE is increased by $\log_2(K)$. If, on the other hand, EDOF subchannels are transmitting in parallel, the system SE should increase by $\mathrm{EDOF} \times \log_2(K)$. Hence, the EDOF can be defined as $\mathrm{EDOF} = (\mathrm{d}/\mathrm{d}\delta)\mathrm{SE}(2^{\delta}P)|_{\delta=0}$ (ref. 35).

References

34. Cover, T. & Thomas, J. A. *Elements of Information Theory* (Wiley, 2012).
35. Shiu, D.-S., Foschini, G. J., Gans, M. J. & Kahn, J. M. Fading correlation and its effect on the capacity of multielement antenna systems. *IEEE Trans. Commun.* **48,** 502–513 (2000).

nature photonics

SUPPLEMENTARY INFORMATION

DOI: 10.1038/NPHOTON.2015.214

Capacity limits of spatially multiplexed free-space communication

1. Canonical LOS System

A. Single-Lens System

First, we consider an LOS system having a single thin positive lens between the transmitter and the receiver. The transmitter aperture is imaged from the object plane O to the image plane I_1, as shown in Fig. S1.

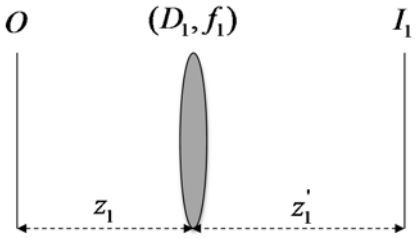

Figure S1: Schematic of an LOS system with a single lens.

The point spread function (PSF) of this imaging system is [1]

$$h_1(x_1', y_1'; x_1, y_1) = \frac{1}{\lambda^2 z_1 z_1'} \exp\left[i \frac{\pi}{\lambda z_1} (x_1^2 + y_1^2) \right] \exp\left[i \frac{\pi}{\lambda z_1'} (x_1'^2 + y_1'^2) \right]$$

$$\times \int P_1(x, y) \exp\left\{ -i \frac{2\pi}{\lambda z_1'} [(x_1' - K_1 x_1)x + (y_1' - K_1 y_1)y] \right\} dxdy ,$$

where $K_1 = -z_1' / z_1$ is the magnification, $P_1(x, y) = \mathrm{circ}(2\sqrt{(x^2 + y^2)} / D_1)$ is the aperture function, and D_1 is the lens diameter. If the spot sizes on the object and image planes are small, the two phase factors can be ignored (paraxial approximation), and the PSF becomes

$$h_1(x_1', y_1'; x_1, y_1) = \frac{1}{\lambda^2 z_1 z_1'} \int P_1(x, y) \exp\left\{ -i \frac{2\pi}{\lambda z_1} [(x_1' - K_1 x_1)x + (y_1' - K_1 y_1)y] \right\} dxdy$$

Therefore, the imaging system can be regarded as a linear shift-invariant system and can be conveniently analyzed in the frequency domain. We focus on this regime because, again, it is the most favorable regime for OAM multiplexing, since non-paraxial phase distortion affects OAM multiplexing but not SMM or LOS MIMO. If the field amplitude in the object plane is $E_0(x_0, y_0)$ with a spectrum $F_0(\nu_x, \nu_y)$ given by its spatial Fourier transform, the spectrum of the field in the image plane I_1 is

DOI: 10.1038/NPHOTON.2015.214

$$F_1(\nu_x,\nu_y) = P_1(-\lambda z_1\nu_x, -\lambda z_1\nu_y)F_0(K_1\nu_x, K_1\nu_y)$$

$$= circ(-\lambda\sqrt{\nu_x^2+\nu_y^2}K_1 / NA_1)F_0(K_1\nu_x, K_1\nu_y),$$

where $NA_1 = D_1 / 2z_1$, is the numerical aperture of the lens. The formulation here was used to perform the simulations detailed in the Methods section.

As an example, we present the parameters of a LOS systems with the largest space-bandwidth product considered in the paper, corresponding to $M = \pi NAR_0/\lambda = 20$. We assume an operating wavelength $\lambda = 1.5$ μm, $NA = 0.25$ and $R_0 = M \times 1.9$ μm. On the object plane, the paraxial condition is satisfied for $z_1 \gg R_0^2/\lambda \approx 1$ mm. So we choose $z_1 = 40$ cm and $D_1 = 20$ cm. On the image plane I_1, the paraxial condition requires $(x_1'^2 + y_1'^2) = (z_1' R_0 / z_1)^2 \ll \lambda z_1'$, i.e., $z_1' \ll \lambda(z_1/R_0)^2 = \lambda[(D_1/2)/NA/R_0)]^2 = 166$ m. If we choose $z_1' = 40$ m, the focal length is $f_1 = 39.2$ cm. Similarly for a millimeter-wave system with $\lambda = 2.0$ mm, $NA = 0.25$, and $R_0 = M \times 3.8$ mm, the paraxial approximation requires $z_1 \gg 2.8$ m and $z_1' \ll 35$ m, and one can choose $D_1 = 5$ m, $z_1 = 10$ m, $z_1' = 15$ m and $f_1 = 6$ m.

B. Dual-Lens System

Next, we consider a LOS system having thin positive lenses at both the transmitter and the receiver, as shown in Fig. S2. The transmitter aperture is imaged from the object plane O to the image plane I_1 through the transmitter lens, then is imaged from I_1 to the receiver aperture plane I_2.

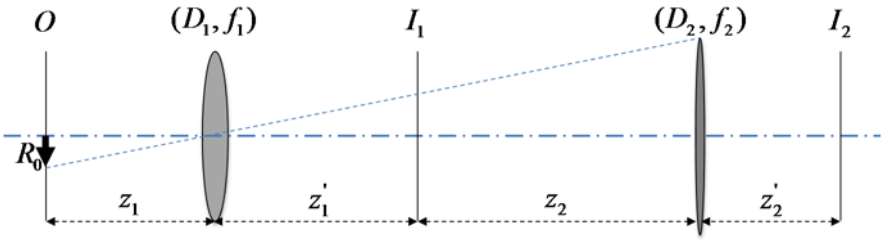

Figure S2: Schematic of a LOS system with lenses at the transmitter and the receiver.

Using the results above, the spectrum at the image plane I_2 is

$$F_2(\nu_x,\nu_y) = circ(-\lambda\sqrt{\nu_x^2+\nu_y^2}K_2 / NA_2)F_1(K_2\nu_x, K_2\nu_y)$$

$$= circ(-\lambda\sqrt{\nu_x^2+\nu_y^2}K_2 / NA_2)circ(-\lambda\sqrt{\nu_x^2+\nu_y^2}K_1K_2 / NA_1)F_0(K_1K_2\nu_x, K_1K_2\nu_y).$$

If $NA_2 \geq NA_1 / K_1$,

$$F_2(\nu_x,\nu_y) = circ(-\lambda\sqrt{\nu_x^2+\nu_y^2}K_1K_2 / NA_1)F_0(K_1K_2\nu_x, K_1K_2\nu_y).$$

If $NA_2 \le NA_1 / K_1$,

$$F_2(\nu_x,\nu_y) = circ(-\lambda\sqrt{\nu_x^2+\nu_y^2}K_2 / NA_2)F_0(K_1K_2\nu_x, K_1K_2\nu_y)$$

A LOS system should be designed to match the numerical apertures so that $NA_2 = NA_1 / K_1$ to avoid clipping the beam in order to maintain the orthogonality among the spatial modes used for multiplexing. In this case, the previous two equations are identical. Hence, an LOS system with lenses at the transmitter and the receiver is equivalent to a single-lens system with an effective numerical aperture (NA_1 or K_1NA_2) and an effective magnification K_1K_2.

To maintain the space-bandwidth product of the two-lens system, the distance between the two lenses should be short enough that $R_0(z_1^{'}+z_2)/z_1 \le D_2/2$, as in Fig. S2, to avoid beam clipping at the receiver lens. In terms of the total transmission distance $z_1'+z_2$, this condition is $(z_1^{'}+z_2) \le z_1D_2/2R_0 \approx f_1D_2/2R_0$, showing that achieving long transmission distance requires that the diameter of the receiver lens scale linearly with transmission distance. These requirements for achieving long transmission distance apply to all the multiplexing methods discussed in this paper.

C. Parabolic-Index Fiber

As discussed in the previous subsection, a system of two lenses is equivalent to the single-lens canonical system with proper choice of numerical aperture and magnification. As a consequence, a concatenation of any number of lenses is equivalent to the single-lens canonical system. The single-lens canonical system can also describe a fiber with a parabolic index profile

$$n(r) = \begin{cases} n_1\left[1-2\Delta(r/a)^2\right]^{1/2} & (r \le a) \\ n_2 & (r > a) \end{cases},$$

where a is the core radius and $\Delta = (n_1^2 - n_2^2)/2n_1^2$ is a normalized refractive index difference. A full-pitch fiber segment of length $L = \pi a\sqrt{2/\Delta}$ (typically several mm) forms a unit-magnification non-inverting imaging system, while a half-pitch segment of length $L/2$ forms a unit-magnification inverting system. A fiber of length $l \le L/4$ is equivalent to a thin positive lens of focal length $f(l) = \left[n_1(\sqrt{2\Delta}/a)\sin(l\sqrt{2\Delta}/a)\right]^{-1}$ [2]. A long fiber can be viewed as a concatenation of many unit-magnification imaging systems, at most one positive lens with focal length $f(L/4)$, and at most one positive lens with focal length $f(l)$, $l < L/4$. With proper placement of the transmitter and receiver apertures, the parabolic-index fiber is described by the single-lens canonical system.

DOI: 10.1038/NPHOTON.2015.214

2. Signal-to-Noise Ratio

In Fig. 3 of the paper, we plot spectral efficiency and EDOF as a function of the system signal-to-noise ratio $SNR = P/\sigma^2$ where P is the total transmitted power in all subchannels and σ^2 is the received noise power per subchannel. Here, we describe system designs achieving the SNR values considered in Fig. 3.

We assume a symbol rate R_s = 10 Gbaud. We consider an optical system at wavelength λ = 1.5 μm, assumed to be local oscillator shot-noise-limited, so the SNR equals the number of transmitted photons per symbol [3], which is equivalent to choosing $\sigma^2 = hcR_s/\lambda = -59$ dBm, the power corresponding to one photon per symbol. We consider a millimeter-wave system at λ = 2.0 mm, assumed to be thermal-noise-limited at temperature T = 300 K so $\sigma^2 = -74$ dBm [4]. We compute the average transmitted power per subchannel P/Q, where Q, given by (5), is the total number of subchannels used by a given spatial multiplexing method at a given SNR.

In Fig. S3, we plot the average transmitted power per subchannel P/Q for the four spatial multiplexing methods as functions of the system SNR for space-bandwidth products described by (a) $M = 3$, (b) $M = 9$ and (c) $M = 21$. In each plot, the left and right axes quantify average powers for the optical and millimeter-wave systems, respectively, and the black dashed horizontal lines denote the noise powers per subchannel, equal to –59 dBm and –74 dBm, respectively. At $M = 3$, all four methods use nearly the same average power per subchannel. By contrast, at $M = 21$, OAM uses more power per subchannel yet achieves lower spectral efficiency than SMM or LOS MIMO, a consequence of having smaller EDOF than the latter two methods. The vertical distances between the curves vary with SNR because we compute Q using (5), which varies with SNR, as opposed to values of Q estimated by (6)-(8).

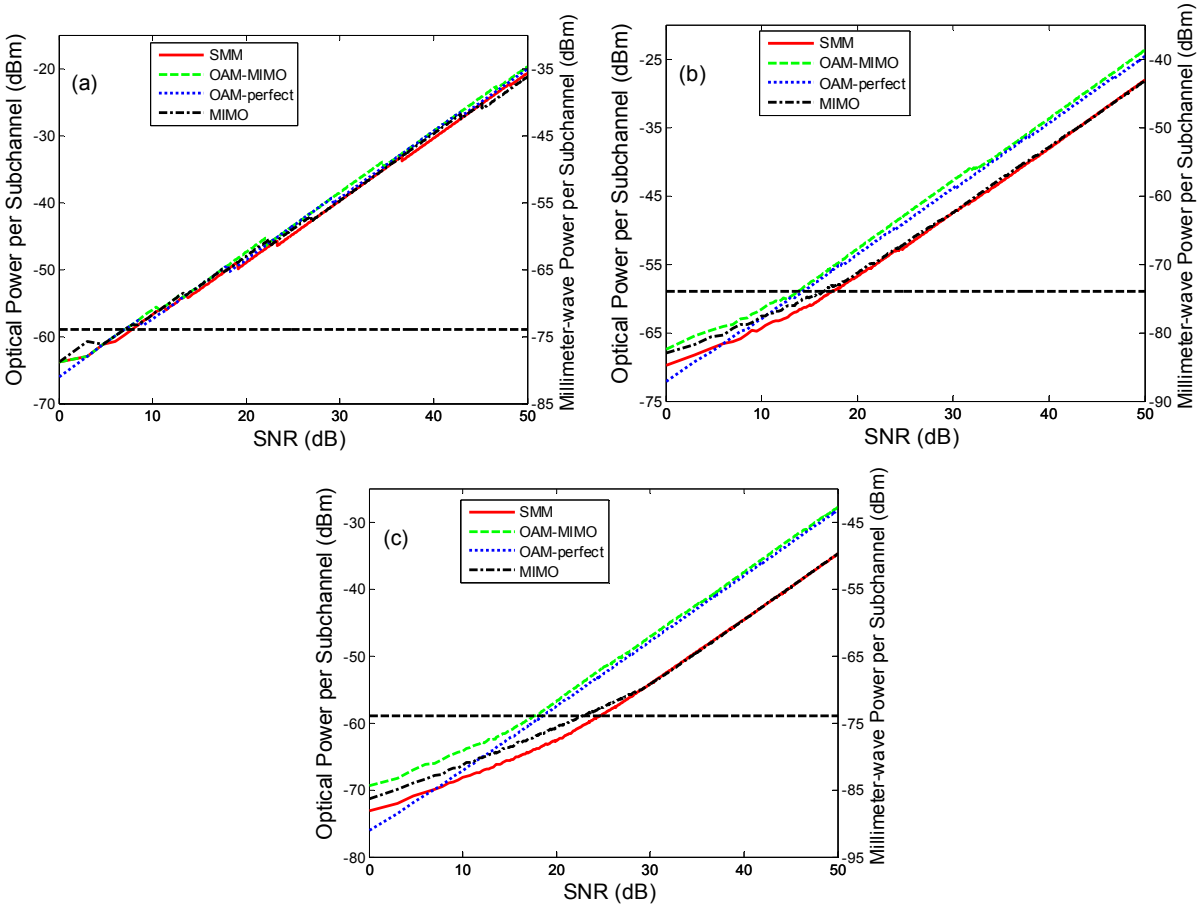

Fig. S3: Average transmitted power per subchannel P/Q as a function of $SNR = P/\sigma^2$ for optical regime (left axis) and millimeter-wave regime (right axis) for space-bandwidth products described by (a) $M = 3$, (b) $M = 9$ and (c) $M = 21$. A symbol rate of 10 Gbaud is assumed. The black dashed horizontal lines correspond to the equivalent noise power per subchannel σ^2.

3. OAM and LG Mode Multiplexing and Demultiplexing using Structured Directional Couplers

Modal multiplexing for OAM transmission was initially based on mode conversion and passive combining, for example, q-plates [5] for mode conversion and beam splitters for combining. Such methods are lossy, due to passive combining. Efficient methods for sorting OAM modes have been developed recently [6-8]. The fiber mode-division multiplexing research community has developed lossless mode multiplexing methods, such as photonic lanterns [9], reconfigurable add/drop mode multiplexers [10], and structured directional couplers [11, 12]. Here we show that structured directional couplers can be used for OAM and LG mode multiplexing in LOS transmission.

DOI: 10.1038/NPHOTON.2015.214

In a structured directional coupler, the input single-mode fiber (SMF) can be selectively coupled to one of the two degenerate zero-OAM LP modes depending on the relative orientation of the input SMF and the output multimode fiber (MMF). Two input SMFs can be positioned appropriately to excite the two degenerate zero-OAM LP modes with a one-to-one correspondence, as illustrated in Fig. S4 for excitation of the LP_{11a} and LP_{11b} mode. If the input SMFs contain signals A and $\pm jA$ (where multiplication by $\pm j$ represents a $\pm 90^o$ phase shift), the resulting field in the output MMF is the OAM mode $LP_{11a} \pm jLP_{11b}$ with OAM number $l = \pm 1$.

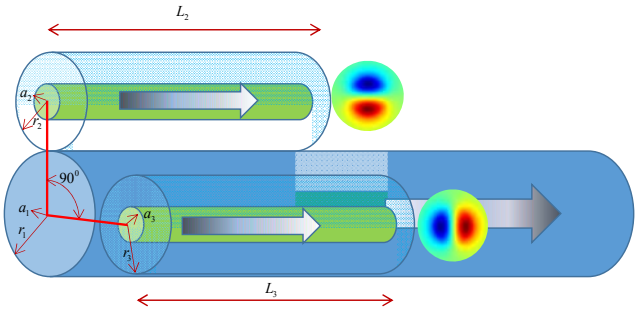

Figure S4: Structured directional coupler. The propagation constant of the two single-mode input fibers match that of the LP_{11} mode the output multimode fiber. The horizontal (vertical) single-mode fiber excites the LP_{11a} (LP_{11b}) mode respectively.

In conjunction with a 2×2 directional coupler, as shown in Fig. S5, a structured directional coupler can couple two input signals into the two degenerate OAM modes of the MMF. A series of such elements can be cascaded to multiplex input signals into all the OAM modes of the MMF. Furthermore, the MMFs can be adiabatically tapered to transform the OAM fiber modes to the corresponding LG modes in free space. Such an OAM multiplexer avoids the combining losses that are present in conversion-plus-combing multiplexers. This lossless OAM multiplexer can be operated in reverse as an ideal OAM demultiplexer.

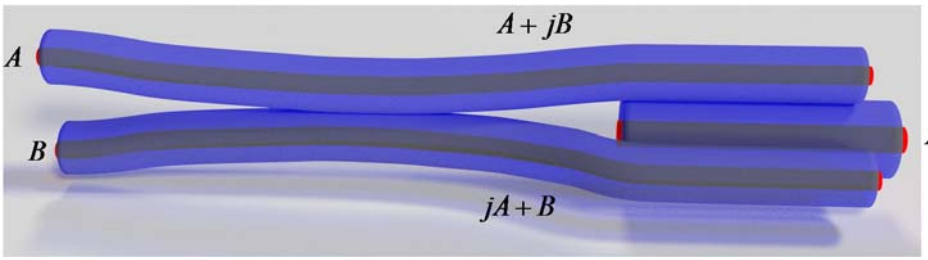

Figure S5: A structured directional coupler and a directional coupler are combined to form a lossless OAM multiplexer or demultiplexer.

4. Effect of Receiver Misalignment on LOS Communication Systems

Since OAM multiplexing can be lossless only if the entire LOS possesses central rotational symmetry, we expect that OAM-multiplexed LOS systems will be sensitive to receiver misalignment. Figure S6 plots the reduction of the EDOF of the different multiplexing-

demultiplexing methods as the receiver lateral misalignment, d , is increased. As expected, the OAM-multiplexed LOS system performs the worst. SMM and conventional LOS MIMO are less sensitive to lateral misalignment because the singular values of the transmission matrix for these two methods are less sensitive to the phase of the received signals than those for OAM multiplexing. Furthermore, using conventional LOS MIMO as an example, when the receiver is misaligned laterally, even though the received power is reduced at one edge, the received power is increased at the opposite edge, reducing sensitivity to receiver lateral misalignment.

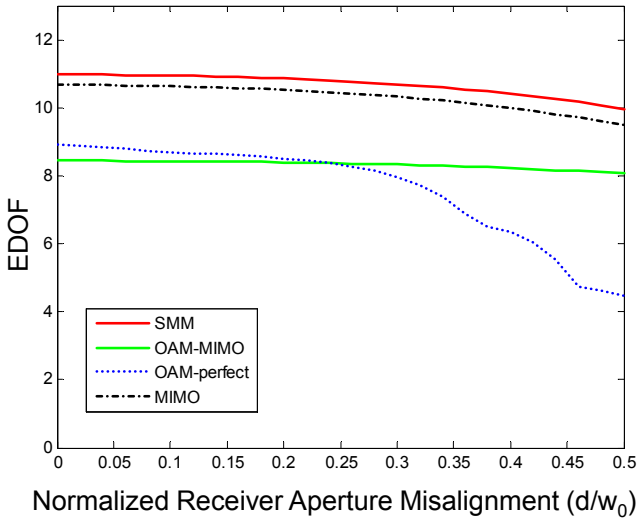

Figure S6: Comparison of the effective degrees of freedom for different multiplexing/demultplexing methods as a function of receiver misalignment for $2R_0 \times 2NA / \lambda = 12 / \pi$ ($M = 3$) and total normalized power *SNR*= 30 dB . OAM multiplexing is the most sensitive to receiver misalignment.

References

1. J. W. Goodman, "Introduction to Fourier Optics," (McGraw Hill, 1996).
2. W. J. Smith, *Modern Optical Engineering* (MaGraw Hill, 2000).
3. E. Ip, A. P. T. Lau, D. J. F. Barros, and J. M. Kahn, "Coherent detection in optical fiber systems," Opt. Express **16**, 753-791 (2008).
4. S. Haykin, "Communication Systems. 1994," (Wiley, New York).
5. E. Karimi, B. Piccirillo, E. Nagali, L. Marrucci, and E. Santamato, "Efficient generation and sorting of orbital angular momentum eigenmodes of light by thermally tuned q-plates," Applied Physics Letters **94**, 231124 (2009).
6. M. Mirhosseini, M. Malik, Z. Shi, and R. W. Boyd, "Efficient separation of the orbital angular momentum eigenstates of light," Nat Commun **4** (2013).
7. M. N. O?Sullivan, M. Mirhosseini, M. Malik, and R. W. Boyd, "Near-perfect sorting of orbital angular momentum and angular position states of light," Opt. Express **20**, 24444-24449 (2012).
8. M. P. J. Lavery, D. Roberston, M. Malik, B. Robenburg, J. Courtial, R. W. Boyd, and M. J. Padgett, "The efficient sorting of light's orbital angular momentum for optical communications," (2012), pp. 85421R-85421R-85427.

DOI: 10.1038/NPHOTON.2015.214

9. S. G. Leon-Saval, A. Argyros, and J. Bland-Hawthorn, "Photonic lanterns: a study of light propagation in multimode to single-mode converters," Opt. Express **18**, 8430-8439 (2010).
10. D. A. B. Miller, "Reconfigurable add-drop multiplexer for spatial modes," Opt. Express **21**, 20220-20229 (2013).
11. B. Huang, C. Xia, G. Matz, N. Bai, and G. Li, "Structured Directional Coupler Pair for Multiplexing of Degenerate Modes," in *Optical Fiber Communication Conference/National Fiber Optic Engineers Conference 2013*(Optical Society of America, Anaheim, California, 2013), p. JW2A.25.
12. N. Riesen, and J. D. Love, "Ultra-Broadband Tapered Mode-Selective Couplers for Few-Mode Optical Fiber Networks," Photonics Technology Letters, IEEE **25**, 2501-2504 (2013).